Rock slope discontinuity extraction and stability analysis from 3D point clouds: application to an urban rock slope

Adrián Riquelme[1], Antonio Abellán[2], Roberto Tomás[3], Michel Jaboyedoff[4]
[1-3] *Departamento de Ingeniería Civil, Universidad de Alicante, Alicante, Spain.*
Email: ariquelme@ua.es; roberto.tomas@ua.es
[2-4] *Center for Research on Terrestrial Environment, University of Lausanne, Lausanne, Switzerland.*
Email: antonio.abellanfernandez@unil.ch; michel.jaboyedoff@unil.es

Abstract

This paper presents an application of a recently developed methodology for the identification and analysis of flat surfaces affecting rock masses using 3D LiDAR point clouds(Riquelme et al., 2013 submited). The used methodology has been applied to calculate the algebraic equations of the different discontinuities of a rock slope through a methodology based on next three steps: (a) local curvature calculation; (b) statistical analysis of the poles and (c) clustering analysis. Once the discontinuities have been identified, their orientations have been employed for evaluating the local stability of different failure mechanisms (wedge and planar) through a classical kinematic analysis.

Key words: *3D point cloud; LiDAR; Discontinuity extraction; Stability analysis*

1. Introduction

The recent development of new remote sensing techniques allows the acquisition of Earth surface datasets in an accurate and quick way. Among these remote sensing techniques, Light Detection and Ranging (LiDAR) technique provides accurate 3D geometries of natural scenes at different scales. The use of terrestrial sensors is especially well adapted for vertical slopes, since the data density is maximized when the Line-of-Sight (LOS) is perpendicular to the scanned topography. Rock slope stability is clearly controlled by several rock parameters as rock strength, discontinuity orientation and dip, persistence, etc. Some of these parameters were recently successfully derived from Terrestrial Laser Scanner (TLS) point clouds. Some approaches calculate the orientation for each node in the triangulated irregular network, TIN (Kemeny and Post, 2003; Lato et al., 2009; Slob et al., 2005) Other authors (García-Sellés et al., 2011; Jaboyedoff et al., 2007; Vöge et al., 2013) proposed the calculation of the local curvature for every point and its coplanar neighbors using the principal component analysis method (hereinafter PCA). Finally, other approaches are based on the searching of volumetric pixels (voxels) and on the subsequent calculation of the planar orientation (Gigli and Casagli, 2011).

In this manuscript we show the application of a new method for 3D point cloud treatment (Riquelme et al., 2013 submited) based on PCA, Kernel Density Estimation and clustering analysis to the extraction of the main sets of discontinuities that intersect a pilot study area located in the urban area of the city of Alicante (SE Spain). Despite the recent advances performed by different research groups on this challenging subject, we consider that still some work have to be done on the extraction of discontinuity sets from 3D point clouds for rock slope stability analysis. For instance, although our algorithm (and most of the scripts appeared in the literature) are normally tested under "ideal" conditions (non-folded surfaces, high enough exposure, datasets acquired from a single station or point of view, reduced or nonexistent sampling biases, etc.). Hence, we considered interesting to test its applicability under more complex conditions as shown in Figure 1 (several stations, several scans, non-planar surfaces, slight folding of the geological layers, etc.).

Figure 1 Picture of the study area.

2. Study area

2.1 *Situation*

The studied rock slope is located in the district of San Blas, Alicante (SE Spain; 38°21'33.83"N / 0°30'32.06"W). The rocky slope extends along the Via Parque urban road, one of the main roads of the city of Alicante, and consists of two subvertical slopes (aprox. 80º) separated by a 4 m horizontal berm with a total height up to 10 m and an orientation N30ºE dipping towards the east. The slope is composed of slightly weathered calcareous marls with a uniaxial compressive strength of 30-32 MPa (Figure 2).

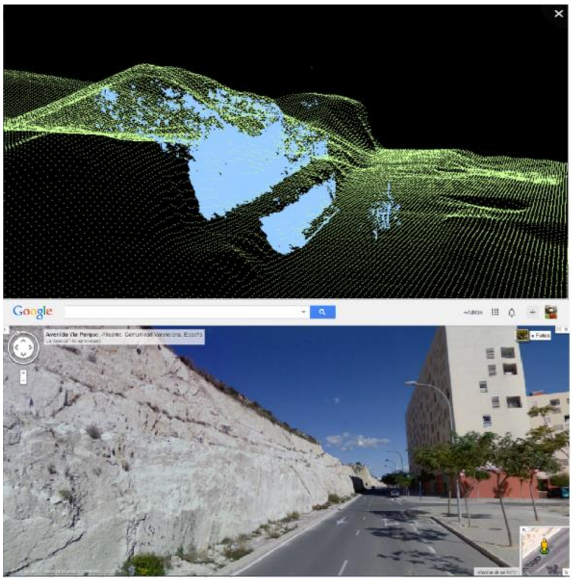

Figure 2 (Above) LiDAR data superimposed to a DEM. (Below) Picture of the study area extracted from Google Street View.

2.2 *3D data acquisition and pre-processing steps*

Fieldwork campaign was developed in summer 2012. The dataset has been built from 10 scans acquired from five different stations. Data pre-processing (vegetation filtering, alignment and merging) has been performed using Polyworks software.

3. **Method for discontinuity characterization**

The method is based on three main steps: calculation of the local curvature, statistical analysis of the plane poles and clustering analysis.

3.1 *Local curvature calculation*

The obtainment of the local curvature for each point was performed through three next stages: (a) Searching the Nearest Neighbours through 'knnsearch' function (Matlab 2013a); (b) Performance of a coplanarity test for a fixed number of neighbours and (c) adjustment of the best fit planes using Principal Component Analysis (PCA) and calculation of the normal vector to this plane.

3.2 *Statistical analysis of the plane poles*

Once all the normal vectors were calculated, we converted all plane poles to stereographic projection. In order to check the statistical significance of each discontinuity set, we calculated the Kernel Density Estimation (KDE) function for each region of the stereographic projection; finally, we calculated the local maxima of the KDE in order to semi-automatically identify the discontinuity sets that affect the rock mass. Each of these maximum values were related to a single family of discontinuities and their associated normal vectors were determined.

3.3 *Cluster analysis*

After the recognition of each of the poles associated to a given DS, we applied a spatial aggregation technique (DBSCAN) for clustering the points belonging to the same discontinuity. The points belonging to a single discontinuity were grouped in order to compute the best fit plane using the PCA. Finally, we performed a tolerance test in order to test if the fitting error was higher than the considered tolerance.

4. **Results: Structural analysis**

4.1 *Visual analysis*

A previous visual analysis was performed on the raw data (Figure 4). This analysis showed the existence of four different discontinuity sets:
- A subvertical discontinuity set that corresponds to the bedding, which is orthogonal to the TLS LOS, and hence, overrepresented in our TLS dataset.
- A subhorizontal discontinuity set, parallel to the LOS.
- Two subvertical discontinuity sets, nearly orthogonal to the bedding plane, also parallel to the LOS.

4.2 *Statistical analysis*

The statistical analysis allowed the identification of four discontinuity sets (DS) as shown in Figure 3.

- J1: sub vertical DS showing a huge density function, due to the high number of points members of this set. This DS shows a high pole dispersion in the stereonet.
- J2: sub horizontal DS. Since the orientation of this family is parallel to J1, its density function may be masked by J1.
- J3 and J4: sub vertical DS which exposure is much reduced; hence, these families are less represented than previous ones.

Dip vector values are shown in Table 1.

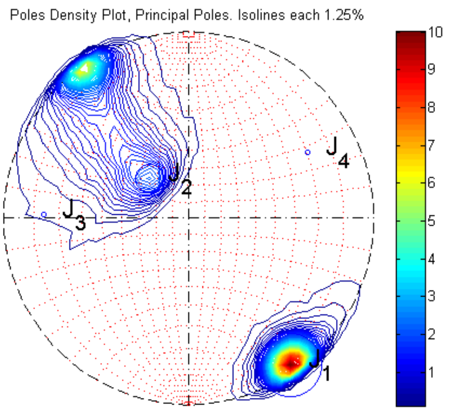

Figure 3 Density data contouring plot of the LiDAR derived normal vector poles.

DS	ω: azimuth º	β: dip º	Density value
J1	325	87	10.15
J2	135	33	2.28
J3	91	76	0.15
J4	241	72	0.05

Table 1 Dip vectors of the principal poles.

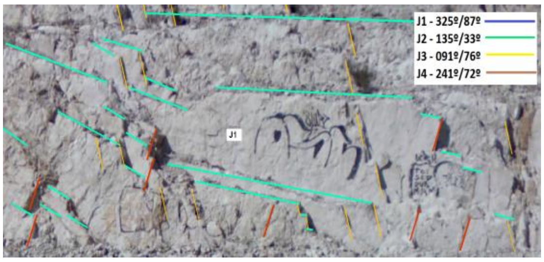

Figure 4 Plot of the discontinuity sets identified by the LiDAR.

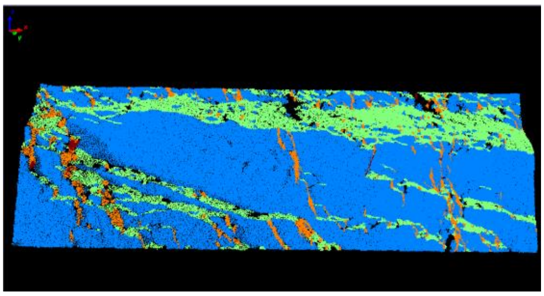

Figure 5 DS derived from LiDAR assigned to each point. J1 in blue, J2 in green, J3 in orange and J4 in brown.

4.3 Cluster analysis

For each cluster, the algebraic plane equation has been calculated. Table 2 shows the statistic of the distance of each point to its assigned cluster plane. The most important fact is that the standard deviation of each DS (σ) has a value between 2 and 8 centimeters. Considering the fact that the area seems slightly folded this is an acceptable result.

DS	Nr of points	ε (m)	σ (m)
1	119,757	$1.90*10^{-4}$	$8.64*10^{-2}$
2	35,628	$4.72*10^{-5}$	$4.27*10^{-2}$
3	10,740	$-1.17*10^{-5}$	$2.64*10^{-2}$
4	765	$5.99*10^{-7}$	$1.75*10^{-2}$
Tot	166,890	$1.46*10^{-4}$	$7.61*10^{-2}$

Table 2 Error fitting analysis. ε: error; σ: standard deviation of the error.

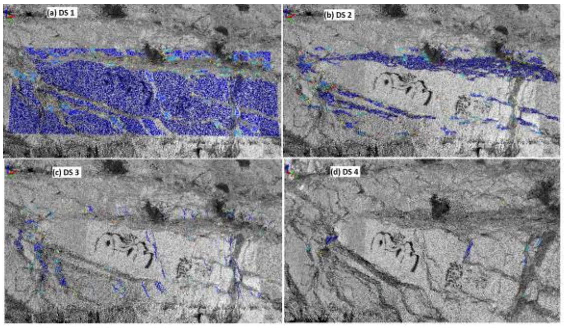

Figure 6 Clusters derived from LiDAR for each discontinuity set.

5. Classical approach using a geological compass

Because the analyzed surface is inaccessible, the discontinuities data acquisition by means of a geological compass has only performed for the road level slope. The later statistical analysis has allowed the identification of three main sets of discontinuities whose orientations are shown in Table 3.

DS	ω: azimuth º	β: dip º
J1’	140	77
J2’	346	10
J3’	242	74

Table 3 Orientations of the recognized discontinuities by means of a classical approach.

Comparing Tables 1 and 3 we can see that the classical approach results are very similar to the LiDAR derived values. Note that the proposed methodology automatically detected four DS, while the classical approach result detected just three of them. This fact is due to several factors, being the most important:

- The classical approach depends critically on the user abilities.
- It is possible that some outcrops do not show clear discontinuity patterns, so the user does not identify them as DS.

6. Discussion and conclusions

We presented a case study on the application of a recently developed algorithm (Riquelme et al., 2013 submited) for the analysis and extraction of rock slope discontinuities. The method allowed us: a) to analyze sets of discontinuities affecting a rock masses in areas of difficult access and b) to identify discontinuity sets not recognizable from fieldwork analysis through a classical approach using geological compass.

In this case study, several sections of the slope were tested in order to analyze the proposed method for discontinuity extraction. When using too big areas, the density function of the J1 DS poles was so high and masked other poorly represented DS (e.g. J2). Our experience showed than a previous user-selection of smaller areas yielded into more accurate results. The classical analysis performed using the geological compass required a user's detection of the DS.
The sampling bias (Lato et al., 2010) appeared in those small enough areas (compared to point density). Furthermore, the extension of the most represented sets should not be excessively larger than the rest. This fact may mask the existence of other DS in the statistical analysis, which should be taken into account in fieldwork planning.

Acknowledgements: This research was founded by the Generalitat Valenciana (project GV/2011/044) and the Swiss National Science Foundation (FNS-138015 and FNS-144040 projects).

References

García-Sellés, D., Falivene, O., Arbués, P., Gratacos, O., Tavani, S., and Muñoz, J. A., 2011, Supervised identification and reconstruction of near-planar geological surfaces from terrestrial laser scanning: Computers & Geosciences, v. 37, no. 10, p. 1584-1594.

Gigli, G., and Casagli, N., 2011, Semi-automatic extraction of rock mass structural data from high resolution LIDAR point clouds: International Journal of Rock Mechanics and Mining Sciences, v. 48, no. 2, p. 187-198.

Jaboyedoff, M., Metzger, R., Oppikofer, T., Couture, R., Derron, M., Locat, J., and Turmel, D., New insight techniques to analyze rock-slope relief using DEM and 3D-imaging cloud points: COLTOP-3D software, *in* Proceedings Rock Mechanics: Meeting Society's Challenges and Demands: Proceedings of the 1st Canada-US Rock Mechanics Symposium, Vancouver, Canada2007, Volume 27, p. 31.

Kemeny, J., and Post, R., 2003, Estimating three-dimensional rock discontinuity orientation from digital images of fracture traces: Computers & Geosciences, v. 29, no. 1, p. 65-77.

Lato, M., Diederichs, M. S., Hutchinson, D. J., and Harrap, R., 2009, Optimization of LiDAR scanning and processing for automated structural evaluation of discontinuities in rockmasses: International Journal of Rock Mechanics and Mining Sciences, v. 46, no. 1, p. 194-199.

Lato, M. J., Diederichs, M. S., and Hutchinson, D. J., 2010, Bias correction for view-limited Lidar scanning of rock outcrops for structural characterization: Rock mechanics and rock engineering, v. 43, no. 5, p. 615-628.

Riquelme, A., Abellán, A., Tomás, R., and Jaboyedoff, M., 2013 submited, A new approach for semi-automatic rock mass joints recognition from LiDAR data: Computers & Geosciences.

Slob, S., van Knapen, B., Hack, R., Turner, K., and Kemeny, J., 2005, Method for Automated Discontinuity Analysis of Rock Slopes with Three-Dimensional Laser Scanning: Transportation Research Record: Journal of the Transportation Research Board, v. 1913, no. -1, p. 187-194.

Vöge, M., Lato, M. J., and Diederichs, M. S., 2013, Automated rockmass discontinuity mapping from 3-dimensional surface data: Engineering Geology, v. 164, p. 155-162.